Visualization of Stem Cell Features in Human Hepatocellular Carcinoma Reveals *In Vivo* Significance of Tumor-Host Interaction and Clinical Course

Shunsuke Muramatsu,[1] Shinji Tanaka,[1] Kaoru Mogushi,[2] Rama Adikrisna,[1] Arihiro Aihara,[1] Daisuke Ban,[1] Takanori Ochiai,[1] Takumi Irie,[1] Atsushi Kudo,[1] Noriaki Nakamura,[1] Koh Nakayama,[3] Hiroshi Tanaka,[2] Shoji Yamaoka,[4] and Shigeki Arii[1]

Hepatocellular carcinoma (HCC) is one of the most aggressive malignancies because of recurrence and/or metastasis even after curative resection. Emerging evidence suggests that tumor metastasis and recurrence might be driven by a small subpopulation of stemness cells, so-called cancer stem cells (CSCs). Previous investigations have revealed that glioma and breast CSCs exhibit intrinsically low proteasome activity and that breast CSCs also reportedly contain a lower reactive oxygen species (ROS) level than corresponding nontumorigenic cells. Here we visualized two stem cell features, low proteasome activity and low intracellular ROS, in HCC cells using two-color fluorescence activated cell sorting to isolate cells with stem cell features. These cells were then analyzed for their division behavior in normoxia and hypoxia, expression of stem cell markers, tumorigenicity, metastatic potential, specific gene expression signatures, and their clinical implications. A visualized small subpopulation of HCC cells demonstrated asymmetric divisions. Their remarkable tumorigenicity in nonobese diabetic/severe combined immunodeficient mice suggested the cancer initiation potential of these HCC CSCs. Comprehensive gene expression analysis revealed that chemokine-related genes were up-regulated in the CSCs subpopulation. Our identified HCC CSCs facilitated the migration of macrophages *in vitro* and demonstrated metastatic potential by way of recruitment of macrophages *in vivo*. In patients who undergo curative operation for HCC, the CSC-specific gene signature in the liver microenvironment significantly correlates with recurrence. *Conclusion*: Based on these findings, the stem cell feature monitoring system proposed here is a promising tool to analyze the *in vivo* significance of CSC microenvironments in human HCCs. (HEPATOLOGY 2013;58:218-228)

Hepatocellular carcinoma (HCC) is one of the most common malignancies and the third leading cause of cancer death worldwide.[1] The primary curative treatment for HCC is surgical resection; however, even after curative resection patient prognosis remains poor because of frequent recurrence and/or metastasis.[2,3] Because cancer stem cells (CSCs) possess self-renewal capacity, multilineage potency, and increased tumorigenicity, it has been hypothesized that CSCs exist as a small population within the bulk tumors and play a critical role in cancer progression, metastasis, and recurrence.[4] Various tools have been reported for identification of the CSC population, including the cell surface markers CD44, CD133, CD90, and ESA/EpCAM.[5-8] In addition, specific stemness properties based on stem cell biology of their

intracellular activities may be useful in identifying CSCs.[9] For example, one property that may be useful in identifying stemness is 26S proteasome activity, which is involved in a diverse array of biological processes, including cell-cycle progression, DNA repair, apoptosis, and protein quality control.[10] Proteasome activity is significantly activated in cancer cells with proliferating and hypermetabolic activities, but generally suppressed in dormant states of stem cells.[11] Vlashi et al.[12] reported that human glioma and breast CSCs were identical to the subpopulation of cells monitored by green fluorescent protein ZsGreen fused to a degron motif of ornithine decarboxylase (ODC), which accumulated within the cell because of low 26S proteasome activity. Stem cells are also characterized by resistance to oxidative stress (superoxide) according to data obtained using the detoxifier system.[13] Hematopoietic stem cells contain a lower level of reactive oxygen species (ROS) than their mature progeny, and these differences are critical for maintaining stem cell function.[14] Human breast CSCs contain lower ROS levels, especially mitochondrial superoxide, than corresponding nontumorigenic cells.[15] In this study, we visualized two stem cell features, low proteasome activity and low ROS levels, in human HCC cells using the ZsGreen-fused degron sequence of ODC and the mitochondrial superoxide indicator MitoSOX Red, respectively. This monitoring system of stemness is a promising tool to elucidate the mechanism of progression and metastasis of human HCC.

Materials and Methods

Cell Culture. HCC cell lines (Hep3B, SK-Hep1, HuH7, and HLF) were purchased from the American Type Culture Collection (Manassas, VA) and the Human Science Research Resources Bank (Osaka, Japan). HuH7, Hep3B, and SK-Hep1 cells were cultured in log-growth phase in 1640 RPMI medium (Invitrogen, Carlsbad, CA), supplemented with 10% fetal bovine serum (Sigma-Aldrich, St. Louis, MO) and Pen/Strep (Sigma) as antibiotics. HLF cells were cultured in Dulbecco's modified Eagle's medium (DMEM; Invitrogen, Carlsbad, CA), supplemented with 10% fetal bovine serum and Pen/Strep, and grown in an incubator with 5% CO_2 at 37°C. Four HCC tumor samples were harvested at the time of surgery. After digestion with type IV collagenase (100 units/mL; Sigma) at 37°C for 15 minutes, the tissues were minced and the cell suspension was passed through a 100-μM nylon mesh and placed into DMEM medium. Cells were cultured in log-growth phase in DMEM medium (Invitrogen), supplemented with 10% fetal bovine serum (Sigma) and grown in an incubator with 5% CO_2 at 37°C.

Retroviral Transduction of the Degron Reporter Into Human HCC Cells. The degron sequence of ODC is known to be directly recognized by the proteasome, which leads to the immediate destruction of the involved protein. A retroviral expression vector pQCXIN-ZsGreen-cODC, containing green fluorescent ZsGreen-labeled degron ODC (Gdeg), was kindly provided by Dr. Frank Pajonk. The vector was transfected into platinum retroviral packaging cells and the retrovirus collected from the supernatant was used to infect HCC cells. Stable transfectants were selected with G418 (Invitrogen), and the accumulation of ZsGreen-degron ODC protein (Gdeg) was monitored by fluorescence microscopy and flow cytometry (FITC channel). Stable transfection was confirmed by exposing the cells to the proteasome inhibitor MG-132 (Calbiochem, San Diego, CA) for 12 hours. The established cell lines (HuH7, Hep3B, HLF, and SK-Hep1) as well as one cell culture line derived from each of the four HCC tissues were successfully engineered to stably express Gdeg. Fluorescence microscopy was performed using Axio-Observer (Carl Zeiss, Oberkochen, Germany), and images were acquired digitally using AxioVision (Carl Zeiss).

Flow Cytometry and Cell Sorting. For the flow cytometry experiments the cell number was evaluated using a FACSCanto II (BD Biosciences), and cell sorting was performed using a FACSAria II (BD Biosciences). HCC cells were washed with phosphate-buffered saline (PBS), then enzymatically dissociated using 0.05% trypsin-EDTA (Invitrogen). Trypsinized cells were suspended in fluorescence activated cell sorting (FACS) buffer and analyzed on a FACSCanto II using FACSDiva software (BD Biosciences). For intracellular ROS analysis, cells were loaded with 5 mM MitoSOX

Red (Invitrogen) at 37°C for 30 minutes and were immediately analyzed using FACSCanto II. Gdeg^{high}ROS^{low} cells represented 0.16%-2.5% of the established HCC cell lines (Supporting Table 1). The percentage of Gdeg^{high}ROS^{low} cells remained the same immediately after isolation by FACS, but increased to approximately 40% after time in culture (Supporting Fig. 4). For surface maker analysis, cells were labeled with allophycocyanin-conjugated antihuman CD44, CD90, EpCAM (BioLegend), and CD133/1 (MACS Miltenyi Biotec) antibodies. Labeled cells were immediately analyzed using FACSCanto II.

Time-Lapse Analysis. After FACS, Gdeg^{high} or Gdeg^{low} HCC cells were plated separately at a density of 10^4 cells in 6-cm dishes and in log-growth phase in 1640 RPMI medium (Invitrogen), supplemented with 10% fetal bovine serum (Sigma) and Pen/Strep (Sigma) as antibiotics. After incubation in 5% CO_2 at 37°C overnight, cell attachment was confirmed. Image analysis was performed using AxioVision and Axio-Observer.

Treatment With Hypoxia or CoCl$_2$. HCC cells were exposed to hypoxic conditions (1% O_2, 5% CO_2, and 94% N_2) in an anaerobic workstation (Hirasawa Works, Tokyo, Japan). Oxygen concentration inside the workstation was constantly monitored by the oxygen sensor (MC-8G-S, Iijima Electrics, Gamagori, Japan) and maintained at 1% during the experiment. Cells (2.5×10^5) were grown with RPMI medium plus 3.5 g/L D-glucose in 10-cm dishes. The proportion of fluorescent cells was measured using FACSCanto II every 2 days. Cells were passaged every 6 days in an anaerobic workstation.

To further assess the effect of hypoxia on HCC cells, cells were treated with 100 μM CoCl$_2$ (Sigma) and/or 10 nM echinomycin (Sigma) added to the medium. After 24 and 48 hours, the proportion of fluorescence cells was measured using FACSCanto II. Chemosensitivity to the anticancer drug fluorouracil (5-FU) was analyzed using Gdeg^{high} HuH7 and unsorted HuH7 cells under these hypoxia-mimicking condition. 5-FU was suspended in the culture media, serially diluted across 96-well microtiter plates (100 μL), and incubated at 37°C with 5% CO_2 for 48 hours. The number of living cells was measured using the MTS assay (Celltiter-Glo Luminescent Cell Viability Assay, Promega, Madison, WI), according to the manufacturer's instructions. The absorbance was read at 490 nm using a multiwell plate reader (Model 550, Bio-Rad, Richmond, CA), with wells containing medium but no cells serving as blank controls. Experiments were independently evaluated in triplicate.

Spheroid Assay. The spheroid assay was performed as described.[16] After FACS, Gdeg^{high} or unsorted cells were plated separately at a density of 1,000 cells in low attachment plates (96-well Ultra Low Cluster Plate; Costar, Corning, NY) and incubated in serum-free DMEM/F12 medium (Invitrogen). For observation by time-lapse microscopy, 6-cm dishes were coated with poly-HEMA (20 mg/mL; Sigma). Image analysis was performed using AxioVision and AxioObserver.

Tumor Xenotransplantation and Tumorigenicity. Female NOD.CB17-PRkdc^{Scid}/J mice aged 4-6 weeks were purchased from Charles River Japan (Kanagawa, Japan). Various numbers of sorted Gdeg^{high}ROS^{low} and unsorted HCC cells, ranging from 1×10^2 to 1×10^5 cells, were each mixed with 100 μL of Matrigel (BD Biosciences) and injected subcutaneously into both flanks of mice under anesthesia. Tumor formation was monitored every 2 days. All *in vivo* procedures were approved by the Animal Care Committee of Tokyo Medical and Dental University (Permission No. 090235).

RNA Extraction and Gene Expression Analysis. Total RNA was extracted from cancer and adjacent noncancerous tissues using the RNeasy kit (Qiagen, Hilden, Germany), and the integrity of obtained RNA was assessed using the Agilent 2100 Bioanalyzer (Agilent Technologies, Palo Alto, CA). All samples had an RNA Integrity Number greater than 5.0. Contaminant DNA was removed by digestion with RNase-free DNase (Qiagen). Complementary RNA was prepared from 2 μg of total RNA using 1-cycle target labeling and a control reagent kit (Affymetrix, Santa Clara, CA). Hybridization and signal detection of HG-U133 Plus 2.0 arrays (Affymetrix) were performed according to the manufacturer's instructions. The microarray datasets of (1) Gdeg^{high}ROS^{low} and Gdeg^{low}ROS^{high} HuH7 cells and (2) 253 tissue samples from HCC patients were normalized separately using the robust multiarray average method found in the R statistical software (v. 2.12.1) together with the Bioconductor package. Estimated gene-expression levels were obtained in log2-transformed values, and 62 control probe sets were removed for further analysis.

Gene Set Enrichment Analysis (GSEA). Biological functions associated with the malignant phenotype in HCC cells were investigated using GSEA v. 2.0.7 with MSigDB gene sets v. 3.0.[17] Probe sets marked as "present" by the Gene Expression Console software (Affymetrix) in at least one Gdeg^{high}ROS^{low} or Gdeg^{low}ROS^{high} HuH7 cell were used for this analysis. Gene set category "C2 CP REACTOME," which is

based on the Reactome database (http://www.reacto-me.org), was used. For analysis of the gene expression profiles obtained from HCC patients, a custom gene set was employed using genes showing more than a 2-fold change between Gdeg^{high}ROS^{low} and Gdeg^{low}ROS^{high} HuH7 cells. Gene sets satisfying both criteria with $P < 0.05$ and a false discovery rate (FDR) <0.05 were considered significant.

Macrophage Migration Assay. To determine whether tumor cells induce macrophage/monocyte chemotaxis, the double chamber migration assay was performed using the RAW264 murine macrophage cell line (RIKEN Cell Resource Center, Tsukuba, Japan). Briefly, the migration of RAW264 cells was assayed using a transwell chamber (24-well plate, 8-μm pore; BD Biosciences, Bedford, MA). In the lower chamber, 7.5×10^4 tumor cells in 0.8 mL of media were seeded and incubated in serum-free media for 72 hours. RAW264 cells (5×10^4 in 0.3 mL serum free media) were then seeded into the upper chamber and incubated at 37°C for 4 hours. RAW264 cells found on the upper surface of the filter were removed using a cotton wool swab. Cells were then fixed with 100% methanol and stained using Giemsa solution and the number of cells migrating to the lower surface was counted. Each experiment was conducted in triplicate and the mean is shown.

Peritoneal Metastasis Model. Peritoneal metastatic potentials of cancer cells were assessed as reported.[18] Briefly, 10^5 Gdeg^{high}ROS^{low} HCC cells or unsorted control cells were injected intraperitoneally into 5-week-old female NOD.CB17-PRkdc^{Scid}/J mice (n = 4 mice per group; Charles River Japan, Kanagawa, Japan). The care and use of animals was in accordance with institutional guidelines. The mice were monitored three times weekly for lethargy, weight loss, and abdominal enlargement. Mice were euthanized by cervical dislocation at 4 weeks and the number and weight of tumor nodules within the peritoneal cavity were counted.

Immunofluorescent Staining. Tissue sections were prepared according to standard procedures. After deparaffinization, slides were incubated in permeabilization buffer (0.2% Triton-PBS) for 30 minutes, followed by incubation in blocking buffer (3% bovine serum albumin [BSA]-PBS) for 1 hour and exposure to the primary antibodies (F4/80 1:200, BioLegend) overnight at 4°C. Sections were then treated for 30 minutes with the secondary antibody Alexa Fluor 568 tetramethylrhodamine isothiocyanate-conjugated anti-rat IgG (1:1,000, Sigma) and Hoechst 33342 solution for nuclear staining diluted in PBS and 3% BSA. After

mounting the slides were visualized with a fluorescent microscope (Carl Zeiss, Germany).

Protein Network Analysis. To reveal functional relationships among genes differentially expressed in Gdeg^{high}ROS^{low} HuH7 cells, the protein interaction network was analyzed. Genes up-regulated or down-regulated more than 1.1-fold between Gdeg^{high}ROS^{low} and Gdeg^{low}ROS^{high}HuH7 cells were included in the network. Protein interaction data obtained from BIND (http://bond.unleashedinformatics.com), Bio-GRID (http://thebiogrid.org), and HPRD (http://www.hprd.org) were downloaded from the ftp site of the National Center for Biotechnology Information (NCBI; ftp://ftp.ncbi.nih.gov/gene/GeneRIF/interactions.gz). The protein interaction network was analyzed using Cytoscape software.[19]

Patients and Tissue Samples. In all, 187 patients underwent curative hepatectomy for HCC from 2004 to 2007 at Tokyo Medical and Dental University Hospital (Tokyo, Japan), and among these, 153 cases were randomly selected for this study. With Institutional Review Board approval, written informed consent was obtained from all patients (Permission No. 1080). Noncancerous liver tissue adjacent to HCC (n = 100) was snap-frozen in liquid nitrogen and stored at −80°C. Patients were followed up with assays for serum alpha-fetoprotein levels and protein induced by vitamin K absence or antagonists-II every month and with ultrasonography, computed tomography, and magnetic resonance imaging every 3 months. Median observation time was 9.86 months.

To divide patients into subgroups based on expression profiles of a particular gene set, gene-set enrichment patterns were analyzed using a method similar to that described by Ben-Porath et al.[20] For each patient, the number of genes that showed more than a 1.1-fold change in expression (either up-regulation or down-regulation) compared to the mean expression levels were counted. Patients who exhibited up-regulation of more than 30% of the genes in the gene set were classified as the high expression group. Likewise, patients who showed down-regulation of more than 30% of the genes in the gene set were classified as the low expression group. Samples that satisfied neither or both criteria above were classified as the moderate expression group. The recurrence-free survival rates among three groups were compared by Kaplan-Meier curves, followed by the log-rank test.

Statistical Analysis. Experimental data are expressed as mean values with 95% confidence intervals (CI) and were compared using a two-sided paired Student's *t* test. Statistical significance was defined as $P < 0.05$.
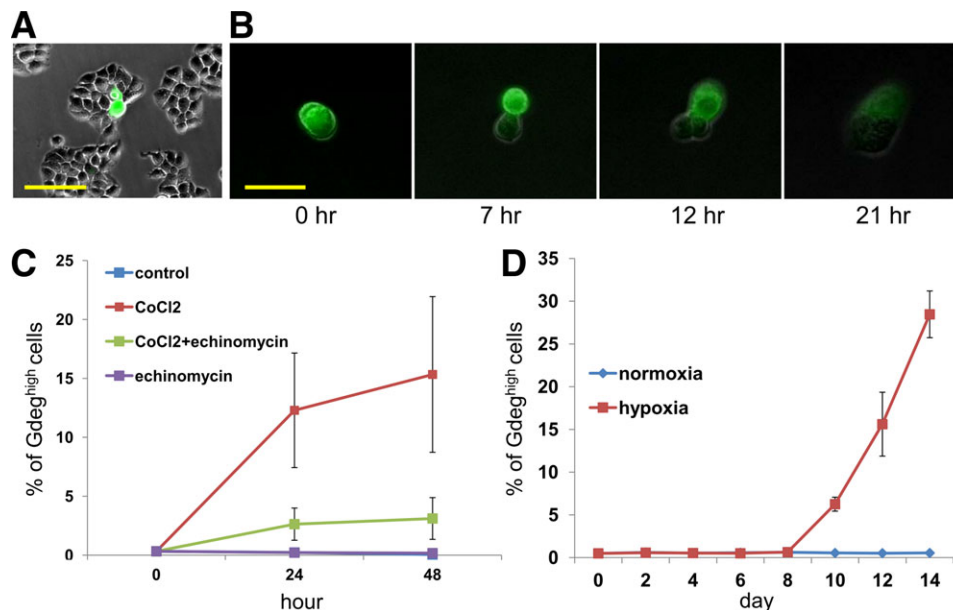
Fig. 1. (A) Frequency of cells with accumulation of Gdeg protein (Gdeg[high]) in human HCC cultures (bar, 100 μm). (B) Asymmetric cell division of the Gdeg[high] HCC observed by time-lapse microscope. Gdeg^{high} HCC cells asymmetrically divided into Gdeg[high] and Gdeg^{low} HCC cells (bar, 50 μm). (C) The alteration of the Gdeg[high] proportion in the unsorted HCC cells after 24-hour and 48-hour treatment of $CoCl_2$ (100 μM) with or without echinomycin (10 nM); results are presented as means $\pm$ standard deviation from triplicate experiments. (D) The alteration of the Gdeg[high] proportion in the unsorted HCC cells under long-term hypoxic conditions (1% O_2); results are presented as means $\pm$ standard deviation from triplicate experiments.

Results

Characterization of CSC Proteasome Activity in Human HCC Cells. Human HCC cells were engineered to stably express ZsGreen-labeled degron (Gdeg) according to the previous report by Vlashi et al.[12] Cells displaying high levels of Gdeg (Gdeg[high]) represented 0.5%-7.5% of the population in human HCC cell lines (Fig. 1A). In contrast, Gdeg^{high} cells represented 0.1% of the population in human primary HCC (Supporting Fig. 1); however, only four generations were passaged without establishment. Isolation of the established Gdeg^{high} cells and Gdeg^{low} cells was performed using FACSAria II (BD Biosciences). As demonstrated by time-lapse microscopy, Gdeg^{high} cells can asymmetrically divide into Gdeg[low] and Gdeg^{high} cells, while Gdeg^{low} cells never divide into Gdeg^{high} cells. These results demonstrate some properties of CSCs and non-CSCs,[21] such as hierarchical division of CSCs and loss of stemness in differentiated non-CSCs (Fig. 1B; Supporting Video 1). In addition, the spheroid assay revealed that Gdeg^{high} cells form slightly larger spheroids than unsorted cells (Supporting Fig. 2).

Effects of Hypoxia on HCC CSCs. Since pluripotent potentials in embryonic stem cells can be efficiently maintained under low oxygen levels[22] and hypoxia can contribute to CSC maintenance,[23] the effects of hypoxic conditions in unsorted HCC cells

transfected with Gdeg were analyzed. The proportion of Gdeg^{high} HCC cells significantly increased after 48-hour treatment with $CoCl_2$, an agent mimicking the activation of hypoxia-inducing factor (HIF).[24] The effects of $CoCl_2$ were blocked by echinomycin, a molecule inhibiting HIF-1 DNA binding activity (Fig. 1C) that has recently been reported to eradicate serially transplantable human acute myeloid leukemia (AML) in xenogeneic models by preferential elimination of CSCs.[25] The effects of long-term hypoxic treatment (1% O_2) were also analyzed in the unsorted HCC cells. Gdeg^{high} cells represented 0.5% of the population on Day 1, but significantly increased to 28.0% on Day 14 (Fig. 1D). Similar to previous reports showing that CSCs are usually resistant to the conventional chemotherapy,[9] Gdeg^{high} cells also demonstrated chemoresistance compared to unsorted cells under hypoxia conditions (Supporting Fig. 3). These results are consistent with reports showing that hypoxic conditions serve as a stimulus to reprogram cells towards normal stem cells and CSCs.[22,23]

CSCs Property of the HCC Subpopulation With Low Intracellular ROS Levels and Low Proteasome Activity. Gdeg^{high} cells had a lower concentration of ROS than the unsorted cells based on the intracellular concentrations of MitoSOX Red staining. Intracellular ROS-positive cells (ROS[high]) accounted for 71.0% $\pm$ 8.22% of the unsorted HuH7 HCC cells, but only
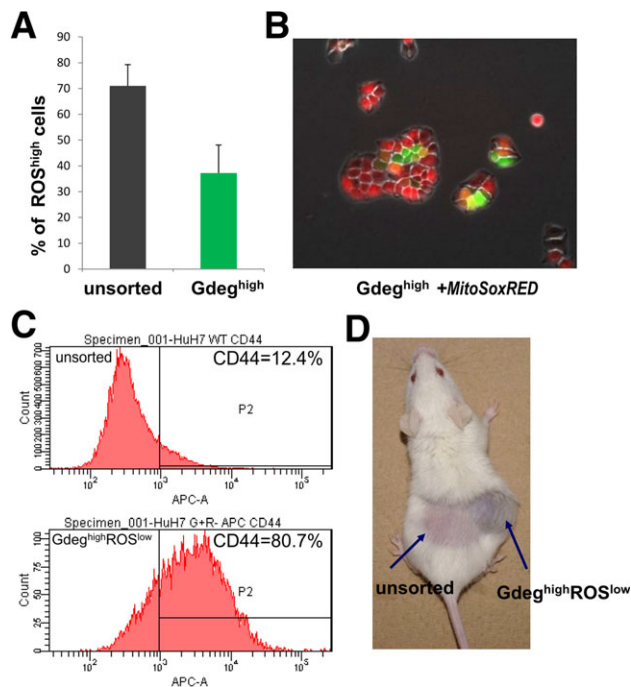
Fig. 2. (A) The proportion of ROS-positive cells (ROS[high]) in unsorted HCC cells (left) and the sorted Gdeg^{high} HCC cells (right) determined by FACS analysis with MitoSOX Red staining; results are presented as means ± standard deviation from triplicate experiments ($P < 0.05$). (B) Gdeg[high] and Gdeg^{high} HCC cells stained with MitoSOX Red; (C) Flow cytometry histogram showing expression of CD44 positive cells in the Gdeg[high]ROS^{low} HuH7 cells (80.7%) and unsorted HuH7 cells (12.4%). (D) Tumorigenicity analysis using NOD/SCID mice; a tumor nodule was detected at the inoculation site of 10^2 Gdeg[high]ROS^{low} HCC cells, but not at the inoculation site of the unsorted cells.

37.2% ± 10.8% within the Gdeg[high] HuH7 cell population ($P < 0.05$). The Gdeg[high] group also contained a subpopulation of cells with low intracellular ROS levels (Gdeg[high]ROS[low]) (Fig. 2A).

To determine whether Gdeg[high]ROS^{low} HCC cells might possess certain stem cell-like properties, the expression of stem cell surface markers, CD133,[5] CD90,[6] EpCAM,[7] and CD44 was analyzed.[8] CD44-postiveness was detected in 80.7% of Gdeg[high]ROS^{low} HuH7 cells, but in only 12.4% of unsorted HuH7 cells (Fig. 2C). EpCAM and CD90 expression were increased in the Gdeg[high]ROS^{low} HLF cells compared to the unsorted HLF cells (EpCAM; 6.0% versus 2.7%, CD90; 55.9% versus 44.6%).

An important test for validating whether cells are CSCs is the identification of a cancer initiation population demonstrated by increased tumorigenicity *in vivo*. Different cell numbers from each population were injected subcutaneously into nonobese diabetic / severe combined immunodeficient (NOD/SCID) mice in numbers ranging from 10^2 to 10^5 cells per injection. Gdeg[high]ROS^{low} HCC cells had higher tumori-

genic capacity than unsorted cells. As few as 10^2 Gdeg[high]ROS^{low} HCC cells could form a subcutaneous tumor (Fig. 2D, Table 1; Supporting Table 2). Cancer initiation frequency was calculated using L-Calc Software[26] (Stem Cell Technologies), and significance was determined by chi-square analysis using ELDA (Walter and Eliza Hall Bioinformatics).[26] The cancer initiation frequency was 1 in 2,083 (95% CI = 739 to 5,867) for Gdeg[high]ROS^{low} HCC cells and 1 in 79,189 (95% CI = 31,651 to 198,128) for unsorted cells ($P < 0.001$). These data validate that CSCs are significantly enriched in the Gdeg[high]ROS[low] subpopulation compared to unsorted HCC cells.

Tumor-Host Interactions of HCC CSCs. Comprehensive gene expression analysis in Gdeg[high]ROS^{low} HCC cells was performed to acquire the CSC gene profile. As described in a previous report,[13] GSEA based on the Reactome database[27] was utilized to determine the biological pathways activated or inactivated in Gdeg[high]ROS^{low} HCC cells. The GSEA demonstrated significant enrichment in 8 gene sets (Supporting Table 3), and the gene set "chemokine_receptors_bind_chemokines" showed the lowest FDR (Fig. 3A). A protein interaction network was then constructed using 12,890 probe sets with at least 10% change in expression levels. To more closely investigate molecular networks associated with chemokines, a subnetwork of 2-hop neighbors from chemokine ligands and receptors including CXCL, CCL, CX3CL, XCL, CXCR, CCR, CX3CR, and XCR family genes was generated (Fig. 3B).

The ability of Gdeg[high]ROS^{low} HCC cells to induce macrophage chemotaxis was determined using a chemotaxis assay and the RAW264 murine macrophage-like cell line (Fig. 3C). Gdeg[high]ROS^{low} HCC cells significantly facilitated RAW264 cell migration compared to their counterparts and unsorted controls (average number of cells that migrated to the lower chamber, Gdeg[high]ROS^{low} HCC cells versus unsorted HCC cells: difference = 192, 95% CI = 61 to 323, $P = 0.0153$, n = 3; Gdeg[high]ROS^{low} HCC cells versus Gdeg[low]ROS^{high} HCC cells: difference = 196, 95%

Table 1. Enhanced Tumor Formation by Gdeg[high]ROS[low] HCC Cells

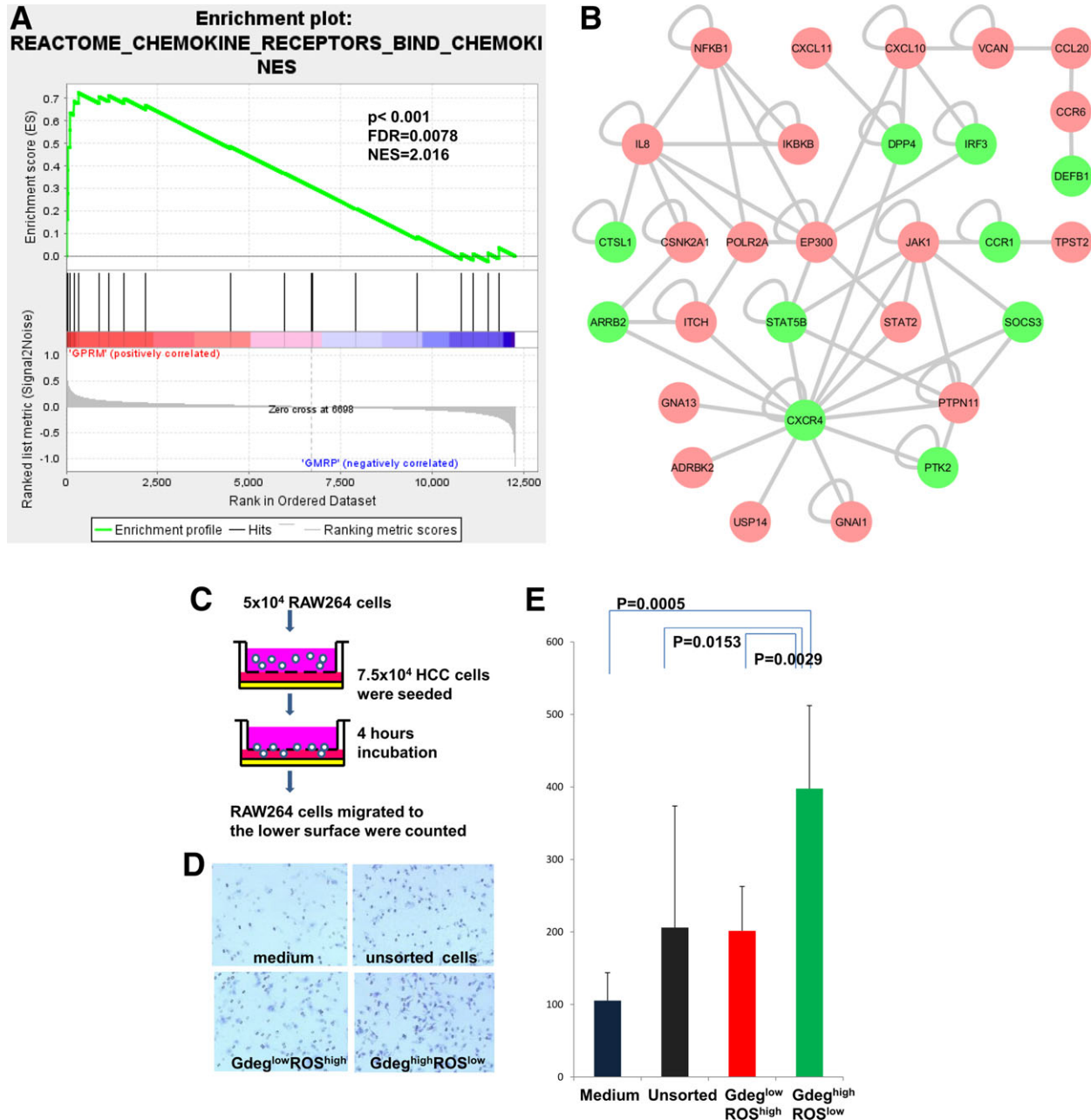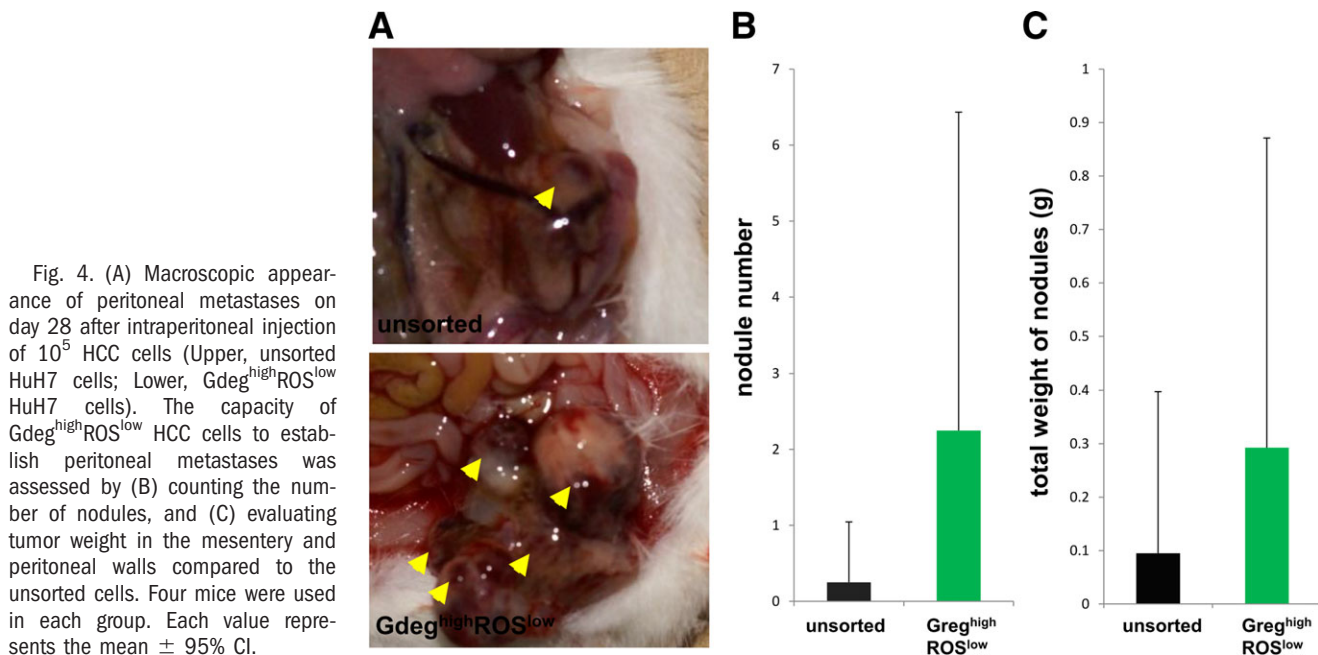| Number of Cells Injected	Fraction (%) of Injected Mice That Developed Tumors	
	Injected With Gdeg[high]ROS[low] Cells	Injected With Unsorted Cells
10^2	3/6 (50%)	0/6 (0%)
10^3	4/6 (66.7%)	1/6 (16.7%)
10^4	5/6 (83.3%)	2/6 (33.3%)
10^5	5/6 (83.3%)	3/6 (50%)

Fig. 3. (A) GSEA evaluation of gene-expression profile associated with Gdeg^{high}ROS^{low} HCC cells; the gene set "chemokine_receptors_bind_-chemokines" showed the lowest FDR ($P < 0.001$; FDR = 0.0078; NES = 2.016). (B) A protein interaction network constructed using 12,890 probe sets with at least 10% change in expression levels; a sub-network of 2-hop neighbors from chemokine ligands and receptors was extracted. (C) Diagram of the double chamber migration assay using a RAW264 murine macrophage-like cell line. (D) Giemsa staining for the RAW264 cells migrating to the lower surface. (E)The number of the RAW264 cells migrated to the lower surface induced by Gdeg^{high}ROS^{low} HCC cells compared to Gdeg^{low}ROS^{high} HCC cells, unsorted HCC cells, and medium. Each experiment was conducted in triplicate, and data are presented as the means ± 95% CI.

CI = 112 to 280, $P = 0.0029$, n = 3, Gdeg^{high}RO-S^{low} HCC cells versus medium: difference = 292, 95% CI = 214 to 370, $P < 0.001$, n = 3) (Fig. 3D,E). Facilitated migration of host macrophages may be associated with niche formation of the HCC CSCs subpopulation.

To investigate whether the HCC cells established *in vivo* metastasis, Gdeg^{high}ROS^{low} or unsorted HCC cells were administered intraperitoneally in a NOD/SCID mouse model, as described previously.[18] Peritoneal metastases were assessed by counting the number of nodules and evaluating tumor weight in the mesentery and peritoneal walls. The tumor weight (average weight of dissemination nodules: Gdeg^{high}ROS^{low} HCC cells versus unsorted HCC cells, difference = 0.197, 95% CI = −0.304 to 0.699, $P = 0.3728$,

Fig. 4. (A) Macroscopic appearance of peritoneal metastases on day 28 after intraperitoneal injection of 10^5 HCC cells (Upper, unsorted HuH7 cells; Lower, Gdeg^{high}ROS^{low} HuH7 cells). The capacity of Gdeg^{high}ROS^{low} HCC cells to establish peritoneal metastases was assessed by (B) counting the number of nodules, and (C) evaluating tumor weight in the mesentery and peritoneal walls compared to the unsorted cells. Four mice were used in each group. Each value represents the mean ± 95% CI.

n = 4; Fig. 4B) and number (average number of dissemination nodules: Gdeg^{high}ROS^{low} HCC cells versus unsorted HCC cells, difference = 2.00, 95% CI = −1.28 to 5.28, P = 0.1857, n = 4; Fig. 4C) of the Gdeg^{high}ROS^{low} HCC cells group were higher than those in the unsorted group. Immunofluorescent analysis revealed that murine macrophages had infiltrated around the Gdeg^{high} HCC cells located at the metastatic tumor margins, indicative of the ability of these cells to recruit macrophages *in vivo* (Fig. 5).

Clinical Implication of the Gene Signature Up-Regulated in HCC CSCs. The clinical implication of the HCC CSC gene signature was retrospectively assessed using liver tissues from patients who received curative resection of HCC. CSC-gene signatures were generated as 43 probe sets using the gene expression profiles up-regulated in Gdeg^{high}ROS^{low} HCC cells

(Supporting Table 4) and revealed a significant correlation between the noncancerous liver gene expressions and the CSC-gene signatures (P = 0.004 and FDR = 0.005; Fig. 6A). CSC-gene signatures were then evaluated with regard to patient outcomes. Patients were divided into three subtypes; high, moderate, and low expression groups, on the basis of expression profiles of the 43 CSC-related probe sets (Fig. 6B). These three groups showed significant differences in recurrence-free survival rates (P = 0.002 by log-rank test; Fig. 6C). High expression was significantly associated with diminished liver function (low albumin and high bilirubin) and tumor number (Supporting Fig. 5). Expression of CSC markers (CD133, EpCAM, CD44, and CD90)[5-8] and biliary/progenitor cell markers (cytokeratin 7 and cytokeratin 19)[28] was also up-regulated in the high expression group (Supporting Fig. 6).
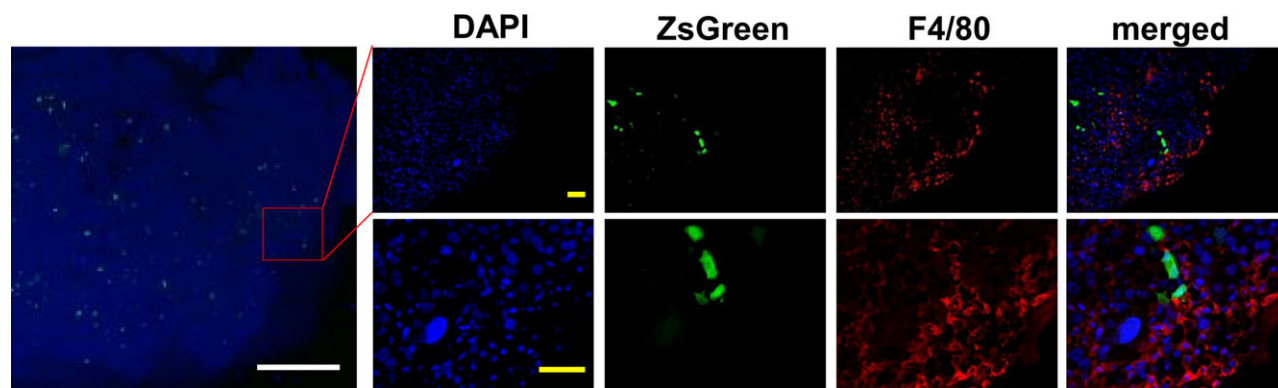

Fig. 5. Immunofluorescence of metastatic tumor sections labeled with antimouse F4/80 (bars, 1,000 μm (white) and 100 μm (yellow)); murine macrophages infiltrated around the Gdeg^{high} HuH7 cells located at the margins of the metastatic tumors.
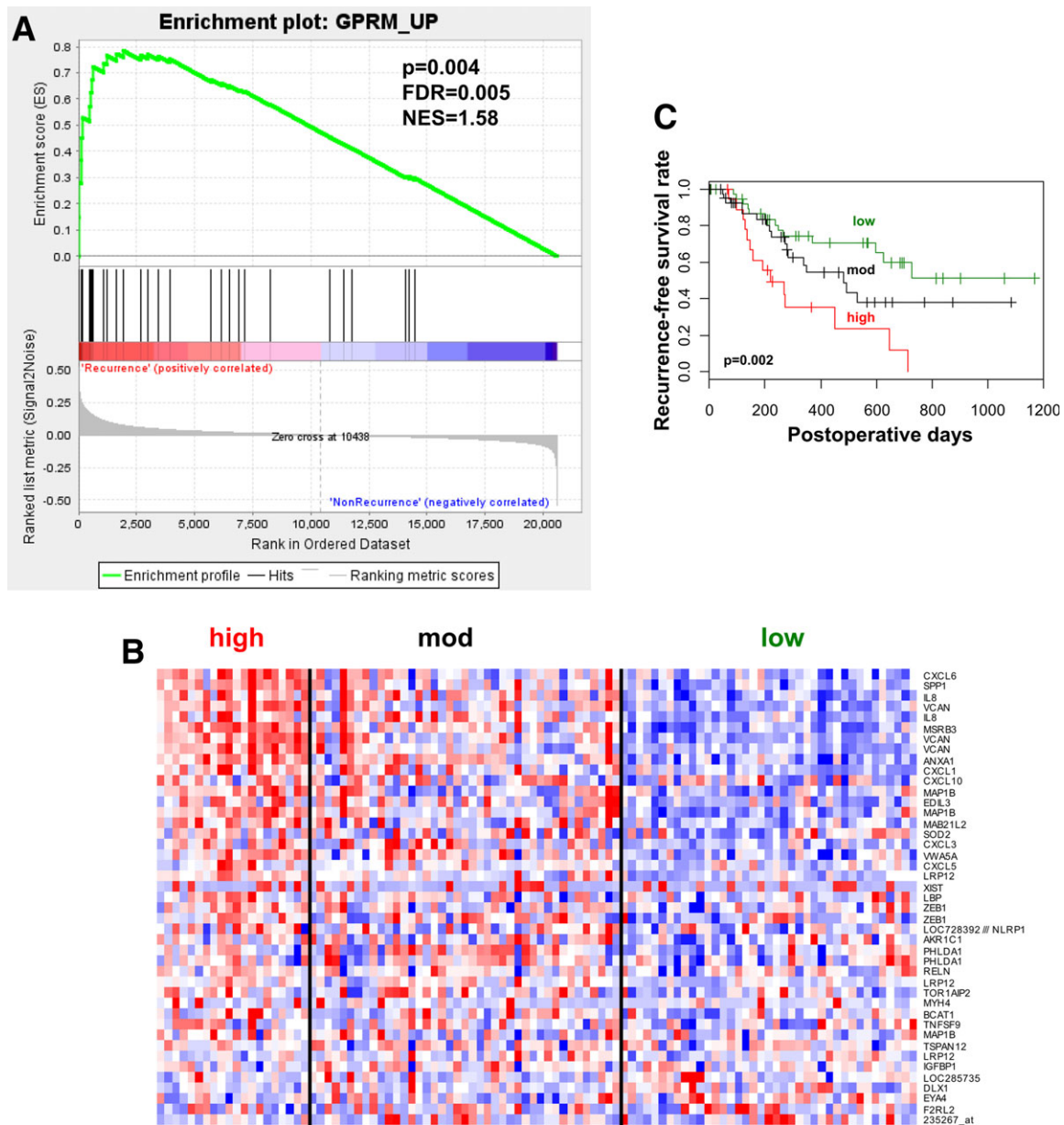
Fig. 6. (A) GSEA evaluation of the adjacent nontumor tissues; a positive correlation was observed between the gene set of Gdeg^{high}ROS^{low} HCC gene signature and noncancerous liver gene expression ($P < 0.004$; FDR $= 0.005$; NES $= 1.58$). (B) Patients were divided into three subtypes based on the expression profiles of 43 up-regulated probe sets of Gdeg^{high}ROS^{low} HCC. (C) A significant correlation was observed between the Gdeg^{high}ROS^{low} HCC gene signature and the recurrence-free survival rates of the patients after curative resection of HCC ($P = 0.002$).

Recently, leukemia CSC-specific gene signatures were revealed as highly independent predictors of patient survival.[29] This gene signature analysis demonstrates the clinical significance of identifying CSC populations in HCC using the stem-cell monitoring system described here.

Discussion

The monitoring system of stemness proposed here visualized two stem cell features, low proteasome activity and low ROS levels, in human HCC. Monitoring HCC proteasome activity revealed that human HCC cells contain a small population of cells that undergo asymmetric division, exhibiting the multipotency and self-renewal of CSCs (Fig. 1B).[20] Next, we showed that $CoCl_2$, an agent mimicking the activation of HIF,[24] increased the proportion of Gdeg^{high} HCC cells, indicative of low proteasome activity, while echinomycin, a molecule that inhibits HIF-1 DNA binding activity, blocked this effect (Fig. 1C). Recently, echinomycin was also reported to eradicate serially

transplantable human AML in xenogeneic models by preferential elimination of CSCs.[25] Similar to $CoCl_2$ treatment, hypoxic conditions also increased the proportion of Gdeg^{high} HCC cells (Fig. 1D), consistent with a previous report indicating that hypoxia serves as a stimulus to reprogram cells towards normal stem cells[22] and CSCs.[23] Additionally, HCC cells had an ROS concentration lower than that of unsorted HCC cells, including a subpopulation of Gdeg^{high} HCC cells (Gdeg[high]ROS[low]), in agreement with a previous report showing that normal stem cells and CSCs contain a lower concentration of ROS than their more mature progeny.[14] Importantly, xenotransplantation experiments revealed that cells with increased tumorigenicity were significantly concentrated in the subpopulation of Gdeg[high]ROS^{low} HCC cells.

An HCC stem cell-specific signature (Supporting Table 4) was identified by genome-wide expression analysis, and GSEA based on the Reactome data base[27] showed that our HCC stem cell system significantly correlated with the chemokine network (Fig. 3A,B; Supporting Table 3). Inflammatory mediators and cells are indispensable components of tumor-host interactions,[30] and studies have shown that cancer cell-secreted factors generate an inflammatory niche hospitable for progression and metastasis of cancer.[31,32] More recent studies have shown that glioma-initiating cells produced inflammatory mediators such as chemokines that induce tumor-associated macrophages to organize the glioma-initiating cells niche.[33] Macrophages are an important component of the tumor-host interaction that controls the survival, migration, and growth of metastatic cells.[34] Our data showed that Gdeg[high]ROS^{low} HCC cells induced macrophage chemotaxis more effectively than their counterparts (Fig. 3E). Furthermore, these cells had a higher capacity for dissemination in an *in vivo* peritoneal metastasis model (Fig. 4B,C). We also found macrophage infiltration around the CSCs located at the margin of the dissemination tumor (Fig. 5), indicative of the ability of HCC CSCs to recruit macrophages *in vivo*.

Recent studies on murine breast CSCs have revealed that the tumor-host interaction plays a critical role in metastatic colonization of cancer cells.[35] It is noteworthy that the tumor-host interaction mediated by HCC CSCs is potentially associated with metastatic initiation in our study. The host gene expression signature of the noncancerous microenvironment is closely associated with prediction of HCC recurrence[36] and lung adenocarcinoma.[37] As a result, the gene expression signature of our HCC stem cells (Supporting Table 4) significantly correlates with the disease-free survival

rate after radical surgery and early recurrence (Fig. 6A). These findings strongly suggest that our HCC stem cell monitoring system is useful in predicting clinical prognosis, and the validity of this system was further confirmed (Fig. 6C).

Our HCC CSCs system, which monitors two stem cell features, is a promising tool to extract and identify CSCs in live bodies and histological specimens. This system demonstrated the presence of a small cell population with an increased capacity to generate dissemination *in vivo*. Clinically, the gene signature specifically expressed in our HCC stem cells significantly correlated with HCC recurrence after radical resection. Taken together, these findings suggest that this stem cell monitoring system could illuminate the *in vivo* significance of CSC-host interactions and microenvironments and improve therapeutic approaches for metastasis and recurrence of aggressive cancers.

References

1. Zhu AX, Duda DG, Sahani DV, Jain RK. HCC and angiogenesis: possible targets and future directions. Nat Rev Clin Oncol 2011;8: 292-301.
2. Arii S, Yamaoka Y, Futagawa S, Inoue K, Kobayashi K, Kojiro M, et al. Results of surgical and nonsurgical treatment for small-sized hepatocellular carcinomas: a retrospective and nationwide survey in Japan. The Liver Cancer Study Group of Japan. HEPATOLOGY 2000;32: 1224-1229.
3. Shrager B, Jibara G, Schwartz M, Roayaie S. Resection of hepatocellular carcinoma without cirrhosis. Ann Surg 2012;255:1135-1143.
4. Reya T, Morrison SJ, Clarke MF, Weissman IL. Stem cells, cancer, and cancer stem cells. Nature 2001;414:105-111.
5. Ma S, Chan KW, Hu L, Lee TK, Wo JY, Ng IO, et al. Identification and characterization of tumorigenic liver cancer stem/progenitor cells. Gastroenterology 2007;132:2542-2556.
6. Yang ZF, Ho DW, Ng MN, Lau CK, Yu WC, Ngai P, et al. Significance of CD90+ cancer stem cells in human liver cancer. Cancer Cell 2008;13:153-166.
7. Yamashita T, Ji J, Budhu A, Forgues M, Yang W, Wang HY, et al. EpCAM-positive hepatocellular carcinoma cells are tumor-initiating cells with stem/progenitor cell features. Gastroenterology 2009;136: 1012-1024.
8. Zhu Z, Hao X, Yan M, Yao M, Ge C, Gu J, et al. Cancer stem/progenitor cells are highly enriched in CD133+CD44+ population in hepatocellular carcinoma. Int J Cancer 2010;126:2067-2078.
9. Clevers, H. The cancer stem cell: premises, promises and challenges. Nat Med 2011;17:313-319.
10. Murata S, Yashiroda H, Tanaka K. Molecular mechanisms of proteasome assembly. Nat Rev Mol Cell Biol 2009;10:104-115.
11. Hernebring M, Brolén G, Aguilaniu H, Semb H, Nyström T. Elimination of damaged proteins during differentiation of embryonic stem cells. Proc Natl Acad Sci U S A 2006;103:7700-7705.

12. Vlashi E, Kim K, Lagadec C, Donna LD, McDonald JT, Eghbali M, et al. In vivo imaging, tracking, and targeting of cancer stem cells. J Natl Cancer Inst 2009;101:350-359.

13. Tanaka S, Mogushi K, Yasen M, Ban D, Noguchi N, Irie T, et al. Oxidative stress pathways in noncancerous human liver tissue to predict hepatocellular carcinoma recurrence: a prospective, multicenter study. HEPATOLOGY 2011;54:1273-1281.

14. Merchant AA, Singh A, Matsui W, Biswal S. The redox-sensitive transcription factor Nrf2 regulates murine hematopoietic stem cell survival independently of ROS levels. Blood 2011;118:6572-6579.

15. Diehn M, Cho RW, Lobo NA, Kalisky T, Dorie MJ, Kulp AN, et al. Association of reactive oxygen species levels and radioresistance in cancer stem cells. Nature 2009;458:780-783.

16. Adikrisna R, Tanaka S, Muramatsu S, Aihara A, Ban D, Ochiai T, et al. Identification of pancreatic cancer stem cells and selective toxicity of chemotherapeutic agents. Gastroenterology 2012;143:234-45.

17. Subramanian A, Tamayo P, Mootha VK, Mukherjee S, Ebert BL, Gillette MA, et al. Gene set enrichment analysis: a knowledge-based approach for interpreting genome-wide expression profiles. Proc Natl Acad Sci U S A 2005;102:15545-15550

18. Tanaka S, Pero SC, Taguchi K, Shimada M, Mori M, Krag DN, et al. Specific peptide ligand for Grb7 signal transduction protein and pancreatic cancer metastasis. J Natl Cancer Inst 2006;98:491-498.

19. Smoot ME, Ono K, Ruscheinski J, Wang PL, Ideker T. Cytoscape 2.8: new features for data integration and network visualization. Bioinformatics 2011;27:431-432.

20. Ben-Porath I, Thomson MW, Carey VJ, Ge R, Bell GW, Regev A, et al. An embryonic stem cell-like gene expression signature in poorly differentiated aggressive human tumors. Nat Genet 2008;40:499-507.

21. Knoblich JA. Asymmetric cell division: recent developments and their implications for tumour biology. Nat Rev Mol Cell Biol 2010;11:849-860.

22. Yoshida Y, Takahashi K, Okita K, Ichisaka T, Yamanaka S. Hypoxia enhances the generation of induced pluripotent stem cells. Cell Stem Cell 2009;5:237-241.

23. Li Z, Bao S, Wu Q, Wang H, Eyler C, Sathornsumetee S, et al. Hypoxia-inducible factors regulate tumorigenic capacity of glioma stem cells. Cancer Cell 2009;15:501-513.

24. Pacary E, Legros H, Valable S, Duchatelle P, Lecocq M, Petit E, et al. Synergistic effects of $CoCl_2$ and ROCK inhibition on mesenchymal stem cell differentiation into neuron-like cells. J Cell Sci 2006;119:2667-2678.

25. Wang Y, Liu Y, Malek SN, Zheng P, Liu Y. Targeting HIF1α eliminates cancer stem cells in hematological malignancies. Cell Stem Cell 2011;8:399-411.

26. Ishizawa K, Rasheed ZA, Karisch R, Wang Q, Kowalski J, Susky E, et al. Tumor-initiating cells are rare in many human tumors. Cell Stem Cell 2010;7:279-282.

27. Croft D, O'Kelly G, Wu G, Haw R, Gillespie M, Matthews L, et al. Reactome: a database of reactions, pathways and biological processes. Nucleic Acids Res 2011;39:D691-697.

28. Durnez A, Verslype C, Nevens F, Fevery J, Aerts R, Pirenne J, et al. The clinicopathological and prognostic relevance of cytokeratin 7 and 19 expression in hepatocellular carcinoma. A possible progenitor cell origin. Histopathology 2006;49:138-151.

29. Eppert K, Takenaka K, Lechman ER, Waldron L, Nilsson B, van Galen P, et al. Stem cell gene expression programs influence clinical outcome in human leukemia. Nat Med 2011;17:1086-1093.

30. Mantovani A, Allavena P, Sica A, Balkwill F. Cancer-related inflammation. Nature 2008;454:436-444.

31. Kim S, Takahashi H, Lin WW, Descargues P, Grivennikov S, Kim Y, et al. Carcinoma-produced factors activate myeloid cells through TLR2 to stimulate metastasis. Nature 2009;457:102-106.

32. Karnoub AE, Dash AB, Vo AP, Sullivan A, Brooks MW, Bell GW, et al. Mesenchymal stem cells within tumour stroma promote breast cancer metastasis. Nature 2007;449:557-563.

33. Yi L, Xiao H, Xu M, Ye X, Hu J, Li F, et al. Glioma-initiating cells: a predominant role in microglia/macrophages tropism to glioma. J Neuroimmunol 2011;232:75-82.

34. Qian B, Deng Y, Im JH, Muschel RJ, Zou Y, Li J, et al. A distinct macrophage population mediates metastatic breast cancer cell extravasation, establishment and growth. PLoS One 2009;4:e6562.

35. Malanchi I, Santamaria-Martínez A, Susanto E, Peng H, Lehr HA, Delaloye JF, et al. Interactions between cancer stem cells and their niche govern metastatic colonization. Nature 2011;481:85-89.

36. Budhu A, Forgues M, Ye QH, Jia HL, He P, Zanetti KA, et al. Prediction of venous metastases, recurrence, and prognosis in hepatocellular carcinoma based on a unique immune response signature of the liver microenvironment. Cancer Cell 2006;10:99-111.

37. Seike M, Yanaihara N, Bowman ED, Zanetti KA, Budhu A, Kumamoto K, et al. Use of a cytokine gene expression signature in lung adenocarcinoma and the surrounding tissue as a prognostic classifier. J Natl Cancer Inst 2007 15;99:1257-1269.